BULLETIN OF THE EARTHQUAKE
RESEARCH INSTITUTE
Vol. 46 (1968), pp. 431-456

21. Lateral Variation of Rayleigh Wave Dispersion Character. Part V. North American Continent and Arctic Ocean.

By Tetsuo SANTÔ,

Earthquake Research Institute and
International Institute of Seismology and Earthquake Engineering.

(Read December 26, 1967.—Received March 31, 1968.)

Summary

Regionalization of the North American Continent, the Arctic Ocean Basin and their surroundings with regard to the group velocity dispersion character of Rayleigh waves (period 20-40 seconds) were made by means of "crossing-path technique." In the North American Continent, dispersion index in the Canadian shield was found to be as low as *5.5*. This result was discussed by comparing with the dispersion data obtained by J. N. Brune et al. It was suggested that Hudson Bay has a thick sediment. In the Arctic Ocean, special dispersion character was not observed along the narrow seismic belt which is considered to be the extension of the Mid-Atlantic Ridge. A dispersion region with extremely high dispersion index of *10* was again confirmed around Novaya Zemlya. The peculiar dispersion character of Rayleigh waves was discovered along the path covering Greenland.

1. Introduction

This is the fifth report on the lateral variation of Rayleigh waves dispersion character in various areas. The method taken is to divide a certain area into several different group velocity dispersion regions in which Rayleigh waves have different group velocity dispersion characters. Group velocity of Rayleigh waves with the periods from 20 to nearly 40 seconds were measured on vertical components of long period seismograms at 25 suitable stations belonging to WWSSN (Table 1) along 36 and 55 paths crossing the North American continent and the Arctic Ocean basin respectively. "Crossing-path technique[1]" was used to divide these two areas into many dispersion regions having different dispersion

1) T. SANTÔ; "Lateral Variation of Rayleigh Wave Dispersion Character. Part II, Eurasia." *Pure and Applied Geophys.*, **62** (1965), 67-80.

Table 1. List of Stations

No.	Station	Region	Latitude	Longitude
7	Albuquerque	New Mexico	34 56 30.0N	106 27 30.0W
12	Atlanta	Georgia	33 26 00.0N	84 23 15.0W
19	Blacksburg	Virginia	37 12 40.0N	80 25 14.0W
22	Bozeman	Montana	45 36 00.0N	111 38 00.0W
27	Copper Mine	Canada	67 50 00.0N	115 05 00.0W
28	College Outpost	Alaska	64 54 00.0N	147 47 36.0W
30	Corvallis	Oregon	44 35 08.6N	123 18 11.5W
32	Dallas	Texas	32 50 46.0N	96 47 02.0W
36	Dugway	Utah	40 11 42.0N	112 48 48.0W
39	Florissant	Missouri	38 49 06.0N	90 22 12.0W
40	Godhavn	Greenland	69 15 00.0N	53 32 00.0W
41	Georgetown	Washington, D.C.	38 54 00.0N	77 04 00.0W
43	Golden	Colorado	39 42 01.0N	105 22 16.0W
52	Kevo	Finland	69 45 21.2N	27 00 45.1E
63	Lubbock	Texas	33 35 00.0N	101 52 00.0W
67	Madison	Wisconsion	43 22 20.0N	89 45 36.0W
79	Nord	Greenland	81 36 00.0N	16 41 00.0W
82	Ogdensburg	New Jersey	41 04 00.0N	74 37 00.0W
83	Oxford	Mississippi	34 30 43.5N	89 24 33.0W
100	Kap Tobin	Greenland	70 25 00.0N	21 59 00.0W
101	State College	Pennsylvania	40 47 42.0N	77 51 54.0W
103	Spring Hill	Alabama	30 41 41.1N	88 08 23.0W
119	Tucson	Arizona	32 18 35.0N	110 46 56.0W
123	Weston	Massachusetts	42 23 04.9N	71 19 19.5W

indexes. Earthquake data according to the Preliminary Epicenter Determination Card by US Coast and Geodetic Survey are given in Table 2, (a) for American and (b) for Arctic paths respectively.

2. Dispersion data in and around the North American Continent

Fig. 1 shows travelling paths of Rayleigh waves along which group velocity dispersion characters were investigated. Fig. 2 gives some examples of dispersion data along these various paths. They lie well parallel to the standard dispersion curves[2], and each dispersion character can approximately be measured to have such dispersion index as is shown by the numeral in parenthesis. This is a neccessary condition which

2) *ibid.*, 1)

Table 2. List of earthquakes

(a) For North American paths

No.	Date	Origin Time (G. M. T.) h m s	Epicenter	M	d	Region
3	Mar. 30 '64	02 18 06.3	56.6N 152.9W	6.7	25	Alaska aftershock
4	Apr. 07	19 28 24.7	55.7N 151.9W	5.6	20	Alaska aftershock
5	08	19 50 16.8	60.4N 145.9W	5.5	10	Alaska aftershock
6	July 21	09 36 16.6	72.1N 130.2W	5.4	33	Laptev Sea
7	May 17	19 26 20.6	35.2N 35.9W	6.5	33	North Atlantic Ocean
9	29	10 17 34.5	60.2N 146.3W	5.6	5	Alaska aftershock
10	30	03 18 08.3	59.5N 148.5W	5.5	20	Alaska aftershock
12	Dec. 17	13 59 25.3	16.0N 96.9W	4.9	36	Oaxacea, Mexico
16	Feb. 14 '65	19 37 17.8	73.0N 6.5E	5.4	33	Greenland Sea
17	May 17 '64	00 50 17.9	59.4N 142.7W	6.5	35	Alaska aftershock
18	19	06 09 04.1	77.7N 18.3W	4.9		Svarbard region
19	July 31	23 45 55.2	86.3N 40.5E	5.3	10	Arctic Ocean
20	Aug. 25	13 47 20.6	78.2N 126.6E	6.5	50	East of Severnaya Zemlya
21	24	21 24 48.0	86.9N 52.0E	4.6	11	North of Franz Josef Land
22	Feb. 14 '65	19 37 17.8	73.0N 6.5E	5.4	33	Greenland Sea
59	Aug. 17	15 15 18.9	72.2N 1.7E		33	Norwegian Sea
67	20	03 56 29.2	63.9N 20.5W		33	Iceland
68	20	02 08 15.8	72.1N 1.4E		33	Norwegian Sea
73	23	04 47 46.6	59.4N 30.2W		33	North Atlantic Ocean

makes it possible to apply "crossing-path technique".

Exclusive dispersion characters were observed, however, on twelve paths from an earthquake 16 in the Greenland Sea. Rayleigh waves crossing Greenland due to this shock (see Fig. 1) offered such special dispersion data as are given in a) and b) of Fig. 3. They deviate from the general tendency of standard curves in the period range of shorter than 25 seconds and seem to lie on rather straight lines.

Quite similar results were actually obtained in the previous case[3] when the regionalization of dispersion regions was performed for the Atlantic Ocean. In that case, five shocks in the Norwegian Sea also sent similar peculiar dispersion data of Rayleigh waves to station 40 (Godhavn) in Greenland along the paths covering the southern part of

3) T. SANTÔ, "Lateral Variation of Rayleigh Wave Dispersion Character. Part III, Atlantic Ocean, Africa and Indian Ocean," *Pure and Applied Geophys.*, **63** (1966), 40-59.

Table 2.

(b) For Arctic area paths

No.	Date	Origin Time (G. M. T.) h m s	Epicenter	M	d	Region
1	May 17 '64	00 50 17.9	59.4N 142.7W	6.5	35	Alaska aftershock
2	June 07	20 30 55.5	45.3N 150.9E	5.0	33	Kurile Is.
3	13	04 20 53.5	53.6N 172.1E	5.1	33	Near Is. Aleutian Is.
4	21	01 33 11.2	51.0N 157.0E	5.7	51	Kamchatka
5	July 14	13 58 28.5	53.3N 159.7E	5.5	40	Near e.c. of Kamchatka
6	21	09 56 16.6	72.1N 130.2E	5.4	33	Laptev Sea
7	31	23 45 55.2	86.3N 40.5E	5.3	10	Arctic Ocean
8	Aug. 17	16 38 44.4	51.5N 177.8E	5.0	42	Rat Is., Aleutian Is.
9	31	23 20 19.4	52.4N 170.7W	5.2	33	Fox Is., Aleutian Is.
10	Dec. 28	17 04 57.0	86.7N 68.7E	5.7	33	North of Franz Josef Land
11	Jan. 01 '65	12 09 12	84.1N 114.8E	4.6	33	North of Severnaya Zemlya
12	29	09 35 25.7	54.8N 161.7E	5.8	33	Near e.c. of Kamchatka
13	31	23 36 13.4	51.2N 178.6E	5.2	33	Rat Is. Aleutian Is.
14	Feb. 7	19 29 23.9	55.2N 165.2E	5.2	20	Kondorsky Is. region
15	Mar. 3 '66	03 25 28.0	48.3N 154.3E	5.9	45	Kurile Is.
17	May 13 '64	03 19 43.2	76.0N 8.2E	4.5	33	Svarbard region
18	19 '64	06 09 04.1	77.7N 18.3E	4.9	33	〃
19	July 07 '64	04 05 27	73.7N 8.6E	4.5	33	〃
20	Aug. 25 '64	13 47 20.6	78.2N 126.2E	6.5	50	East of Severnaya Zemlya
41	24 '64	20 29 11.5	85.9N 20.6E	4.8	33	Svarbard region
42	31 '64	21 22 24.3	86.4N 38.5E	4.9	33	Arctic Ocean
43	Aug. 24 '64	21 24 48.0	86.9N 52.0E	4.6	11	North of Franz Josef Land
143	May 13 '60	16 07 12	55 N 161.5W			Alaska Peninsula
23	Sept. 5 '61	11 34 37.3	59.8N 150.6W	6	44	Kenai Peninsula
27	Aug. 29 '61	14 51 14.2	52.2N 170.8W	5	41	Fox Is. Aleutian Is.
01	June 29 '61	22 01 21.0	85.0N 97.3E	—	11	Severnaya Zemlya
20	Sept. 11 '61	02 46 43.3	51.3N 179.7W	—	15	And. Is. Aleutian Is.
90	Dec. 30 '61	00 39 24.0	52.3N 177.7E	7	52	Rat Is. Aleutian Is.
02	June 26 '61	14 47 26.1	52.4N 174.5E	—	60	Near Is. Aleutian Is.

Greenland. As there are no reasons to suggest any special crustal conditions in the western part of the Norwegian Sea, a thick ice sheet which covers Greenland must be responsible for changing the dispersion data along these paths into such special one.

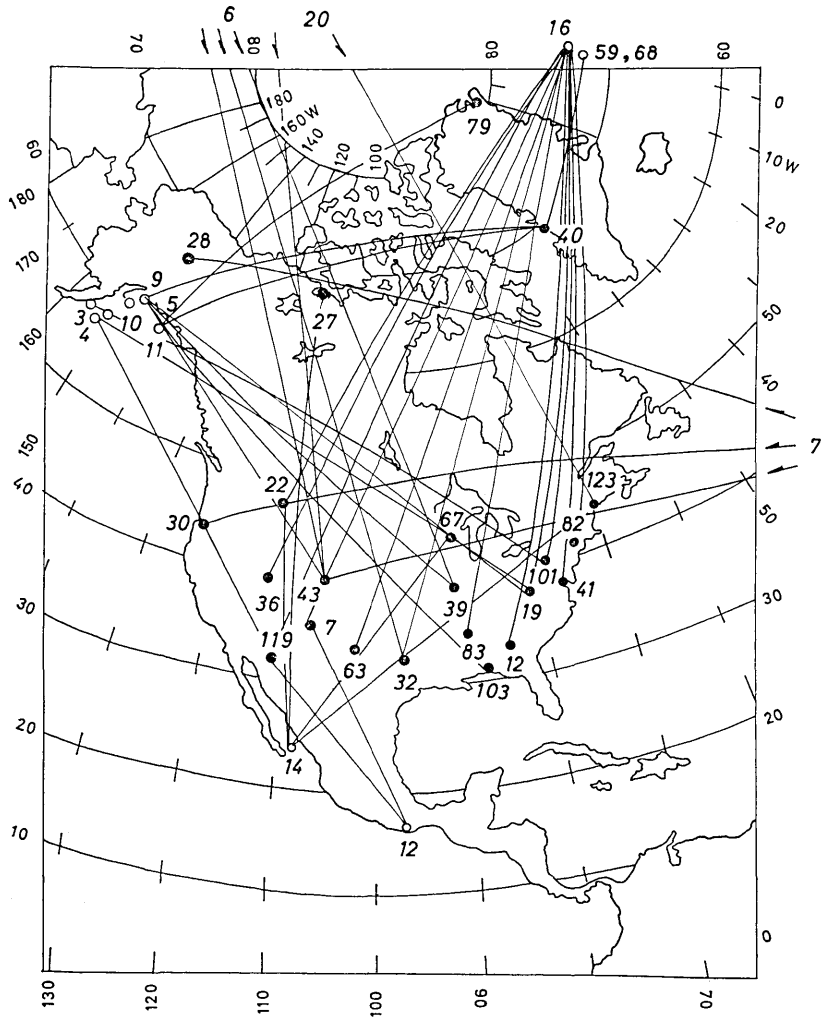

Fig. 1. Travelling paths of Rayleigh waves covering the North American Continent. Filled circles: stations. Open circles: epicenters.

In order to utilize the special dispersion data from the shock 16 to twelve stations for dividing the North American Continent into many standard dispersion regions, the effect of the special dispersion region (we shall call it ***G***), which may exist in Greenland, upon the observed dispersion data must be taken out. That is, the travel-times of Rayleigh waves in that special region (t_G) must be reduced from the travel-times

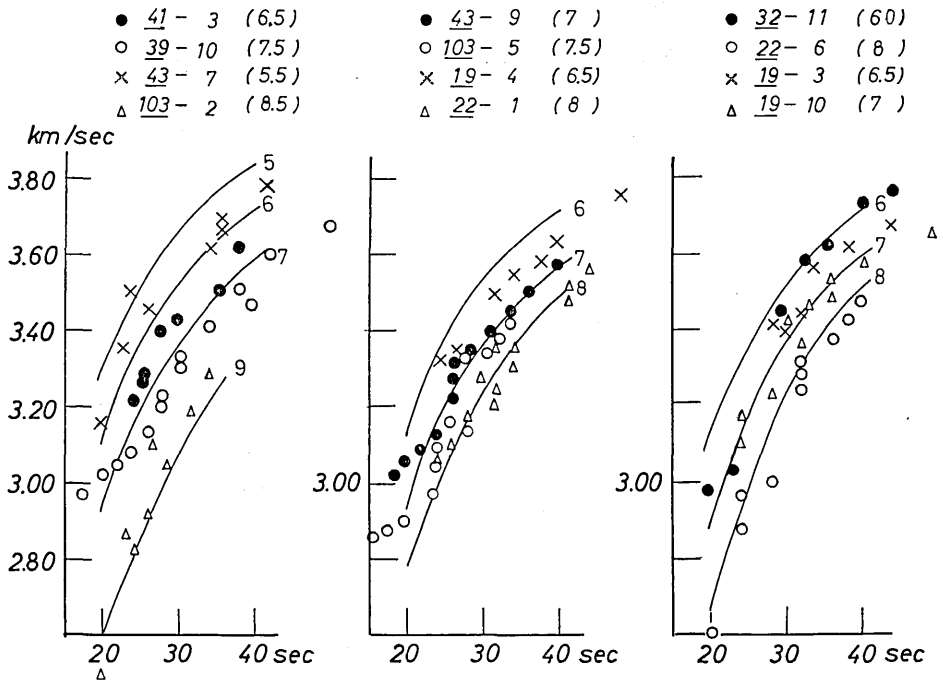

Fig. 2. Some examples of group velocity dispersion data of Rayleigh waves along various paths. Paths are shown by the numerals representing the stations (underlined) and epicenters given in Fig. 1. Values in parentheses mean the dispersion indexes measured by standard dispersion curves. Some standard curves are presented for comparison.

along total path length (t). We have no data of t_G along each path. There are, however, group velocity data along the paths from shocks 59 and/or 68 to the station 40 which were obtained in the previous study. They are 3.40, 3.50, 3.60, 3.70 and 3.80 km/sec for the periods of 20, 25, 30, 35 and 40 seconds respectively. As these two paths are the nearest ones to the twelve paths in the present case, these group velocity data above given may, as an approximation, be used to calculate t_G along every path. $t-t_G$ thus obtained are given in Table 3. Calculated group velocity V' excluding a special segment ***G*** are plotted in (c) and (d) of Fig. 3 against period, which are satisfactorily changed into the values belonging to standard dispersion characters.

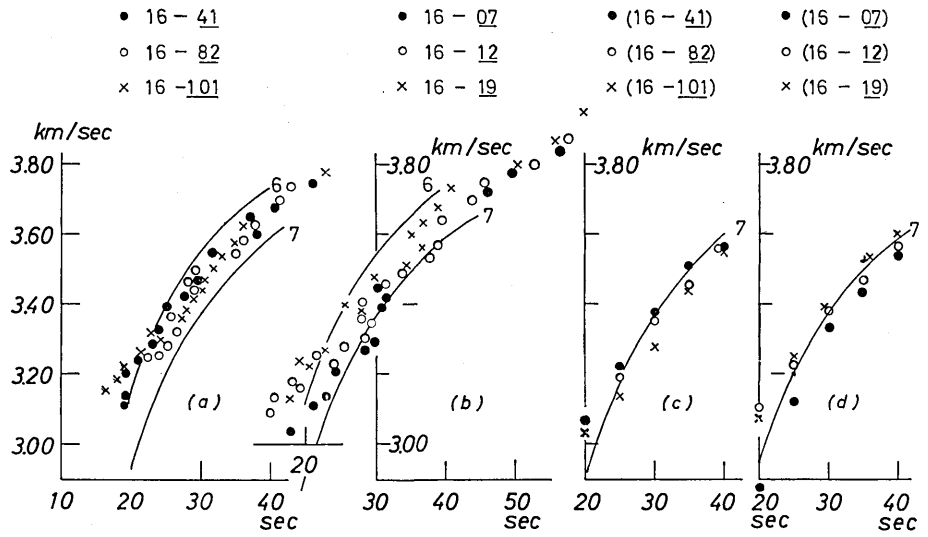

Fig. 3. (a), (b): Dispersion data of Rayleigh waves group velocities along the paths containing Greenland.
(c), (d): Dispersion data along the paths excluding the special region G'.

Table 3. Numerical data for computing the group velocity of Rayleigh waves V′ along the paths excluding a special segment G.

V: Group velocity along total path. t_G: Travel-times of Rayleigh waves in G region computed by G/V_G, in which V_G are the group velocities observed along the paths from the shocks 59, 68 to a station 40. t: Travel-times along the total path.

Path 16-41: Δ=5600 km, G=2500 km

Period (sec)	V (km/sec)	t_G (sec)	t (sec)	t-t_G (sec)	V′ (km/sec)
40	3.66	658	1530	872	3.56
35	3.59	675	1560	885	3.51
30	3.48	694	1610	916	3.38
25	3.34	715	1678	963	3.22
20	3.21	735	1745	1010	3.07

(to be continued)

Table 3. (continued)

Period (sec)	V (km/sec)	t_G (sec)	T (sec)	T-t_G (sec)	V′ (km/sec)
Path 16-82: Δ=5300 km, G=2500 km					
40	3.67	658	1445	787	3.56
35	3.57	675	1487	812	3.45
30	3.46	694	1531	837	3.35
25	3.32	715	1595	880	3.19
20	—	735	—	—	—
Path 16-101: Δ=5400 km, G=2400 km					
40	3.68	631	1481	844	3.55
35	3.59	648	1520	872	3.44
30	3.46	667	1577	913	3.14
25	3.33	685	1638	953	3.03
20	3.22	706	1695	989	3.00
Path 16-07: Δ=6900 km, G=1900 km					
40	3.61	500	1915	1415	3.54
35	3.51	514	1967	1453	3.44
30	3.40	528	2032	1504	3.33
25	3.22	542	2143	1601	3.12
20	3.08	559	2240	1681	2.98
Path 16-12: Δ=6350 km, G=2300 km					
40	3.65	605	1742	1137	3.56
35	3.55	622	1790	1168	3.47
30	3.45	640	1840	1200	3.38
25	3.32	657	1915	1258	3.22
20	3.20	676	1985	1309	3.10
Path 16-19: Δ=5900 km, G=2400 km					
40	3.68	632	1603	991	3.60
35	3.60	649	1640	997	3.53
30	3.48	667	1698	1031	3.39
25	3.35	685	1762	1077	3.25
20	3.20	705	1845	1140	3.07

Table 4. Divided segments Δ_i, travel-times of Rayleigh waves along each segment ti, and the comparison of V_C with V_O. Paths are presented by the numberings of epicenter and station (underlined).

$t_i=\Delta_i/V_i$, where V_i is group velocity of Rayleigh waves with dispersion index i. $\Delta=\sum\Delta_i$, $C=\sum t_i$. O: Observed travel-times of Rayleigh waves along the total path. $V_C=\Delta/\sum t_i$. V_O: Observed group velocity of Rayleigh waves. (Period: 30 seconds)

(a)

Path	{Travel-length Δ_i (in km) / Travel-time t_i (in second)} in segment										Δ	O / C	V_O / V_C	V_O-V_C
	0	*1*	*3*	*5*	*5.5*	*6*	*7*	*8*	*9*	*C*				
3- 41			700 181		1000 280		3400 1010	500 154			5600	1630 1629	3.44 3.44	+0.00
4- 19		300 75	600 155				4100 1220	500 154			5500	1615 1604	3.41 3.43	−0.02
4- 40				800 218	1500 420		1450 432	700 216			4450	1280 1286	3.47 3.46	−0.01
4-119	1000 245	500 125	500 129	300 83			700 208	1000 309			4000	1110 1098	3.60 3.62	−0.02
7- 28		200 50	800 208	1500 410	3600 1008		1600 178	400 123		200 52	7300	2023 2027	3.60 3.60	+0.00
7- 30		200 50	1500 390	400 109	2500 700		1000 297	900 278	400 130	200 52	7100	2010 2006	3.53 3.53	−0.00
7- 43		1200 300	1100 285	200 54			3200 953			200 52	5900	1630 1644	3.62 3.59	+0.03
9- 39							4000 1190	500 154			4500	1344 1344	3.35 3.35	−0.00
9- 43				500 137			550 164	2000 618	500 163		3550	1083 1082	3.28 3.28	−0.00
9-103						700 199	3300 984	1300 401			5300	1590 1584	3.32 3.35	−0.03
10- 19							5250 1560				5250	1560 1560	3.37 3.37	0.00
11- 32			400 104	1200 328	2000 560		4100 1221				7700	2207 2213	3.49 3.48	+0.01
11- 39			700 180	1000 273	3500 980		2100 625				7300	2050 2070	3.56 3.54	+0.02
11- 43				1500 410	1600 449		2700 804	1000 309			6800	1965 1972	3.46 3.45	+0.01
12- 7							300 89	2050 633			2350	725 722	3.23 3.23	−0.00

(to be continued)

Table 4. (continued)

(a)

Path	Travel-length Δi (in km) / Travel-time t_i (in second) in segment										Δ	O / C	V_O / V_C	V_O-V_C
	0	*1*	*3*	*5*	*5.5*	*6*	*7*	*8*	*9*	*C*				
12-119							300	1600	400		2300	713	3.23	0.00
							89	494	130			713	3.23	
14- 22				200			500	700	1000		2400	738	3.31	+0.01
				55			149	277	261			742	3.33	
14- 27				200	1300		450	1100	1800		4850	1464	3.25	−0.02
				55	364		431	339	261			1450	3.24	
14- 67				100		400	1500	600			2630	772	3.41	+0.03
				27		113	455	185				780	3.38	
14-123				100		800	2650	500			4050	1186	3.42	+0.03
				27		228	788	154				1197	3.39	
17- 40					250	600		2300	800		3950	1179	3.35	−0.04
					68	168		684	247			1167	3.39	
17- 79					1200			2000	800		4000	1174	3.40	−0.02
					328			595	246			1169	3.42	
20- 43			800	1200	1700		2180	500			6380	1810	3.53	+0.00
			207	328	476		648	154				1813	3.53	
20-123			400	1400	2700		2000				6500	1831	3.55	+0.01
			103	383	757		595					1838	3.54	

(b)

Path	Travel-length Δi (in km) / Travel-time t_i (in second) in segment										Δ	O / C	V_O / V_C	V_O-V_C
	0	*1*	*3*	*5*	*5.5*	*6*	*7*	*8*	*9*	*G*				
16- 32					1000	600	2550		700	2000	6850	2010	3.41	−0.03
					280	170	759		228	556		1993	3.44	
16- 63					1000		3200		700	2000	6900	2020	3.42	+0.00
					280		952		228	556		2016	3.42	
16- 7					1000		2700	700	600	1900	6900	2020	3.42	+0.00
					280		805	216	191	528		2020	3.42	
11-119					1500		1900	900	1100	1900	7300	2160	3.38	−0.01
					421		564	278	360	528		2151	3.39	
16- 36					2000		500	600	500	1900	6500	1890	3.43	−0.01
					560		477	185	164	528		1889	3.43	
16- 22					1900		1100	700	300	1900	5900	1710	3.45	−0.02
					532		328	213	98	528		1699	3.47	
16- 82				500	1700		1000	600		2500	5300	1528	3.47	−0.04
				136	196		297	185		695		1509	3.51	
16- 41				500	900		1100	600		2500	5600	1609	3.48	−0.03
				136	252		328	185		695		1596	3.51	

(to be continued)

Table 4. (continued)

(b)

Path	Travel-length Δ_i (in km) Travel-time t_i (in second) in segment										Δ	O / C	V_O / V_C	V_O-V_C
	0	*1*	*3*	*5*	*5.5*	*6*	*7*	*8*	*9*	*G*				
16-101				400	1000		950	700		2400	5450	1575	3.46	−0.04
				109	280		283	216		668		1556	3.50	
16- 19				300	1000		1000	1200		2400	5900	1690	3.49	+0.01
				82	280		297	370		668		1697	3.48	
16- 12				200	1500		1850	500		2300	6350	1835	3.46	−0.03
				53	421		551	154		640		1819	3.49	
16- 83					1800		2500			2100	6400	1850	3.46	−0.03
					505		744			585		1834	3.49	

3. Regionalization of the North American Continent into several disperison regions

As in the previous cases for other areas, the North American Continent was divided into several such dispersion regions that the resultant dispersion characters along the whole travelling paths were satisfactorily agreeable with the observed ones. The procedure is to divide every path into such suitable segments of different dispersion regions (Δ_i) that the average group velocity (V_C) along the total path length is calculated within a certain observational value, say ± 0.03 km/sec to the observational value (V_O). For a few paths which partly occupy the northwestern Atlantic Ocean, lengths of segments in the oceanic area were measured based upon the division pattern previously obtained[4]. Lengths of the segments in the Arctic oceanic part are the result of division of the Arctic Ocean basin, which will be described in section 6 of this paper.

Table 4 gives the division data which finally obtained after several trials for Rayleigh wave with the period of 30 seconds. In this table, lengths of segments in each dispersion region Δ_i, travel-times of Rayleigh waves along each segment $t_i(=\Delta_i/V_i)$ are given in the wide column. The data along the paths crossing Greenland are separately given in (b). In this Table 4-(b), *G* means the length of the segment from the epicenter 16 to the eastern coast line of Greenland, and t_G was calculated, as was mentioned before, by dividing *G* by 3.60 km/sec, the group velocity of Rayleigh waves of 30 seconds periods previously obtained along the path from the epicenter 59 or 68 to station 40. The dispersion region *C* in

4) *ibid.*, 3)

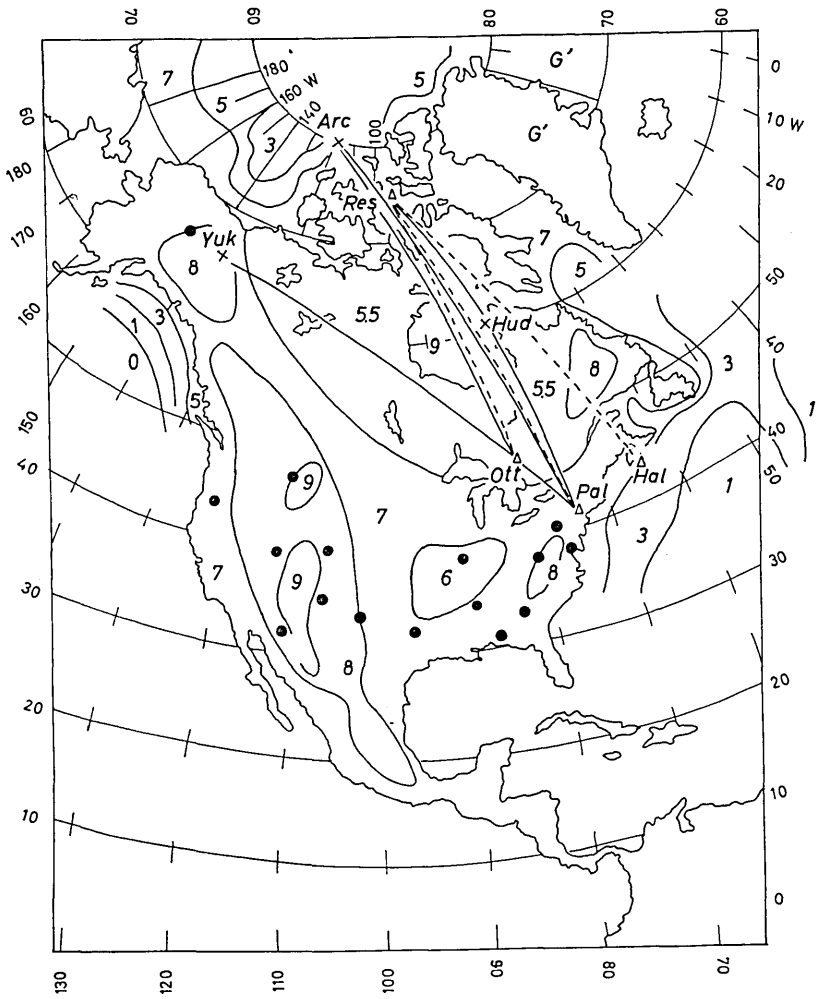

Fig. 4. Division pattern of dispersion region in and around the North American Continent. Travelling paths along which dispersions of Rayleigh waves were investigated by J. Brune et al. are also shown.

(a) means a special region which had been discovered along the Mid-Atlantic Ridge[5]. The resulting group velocity V_C calculated by $\Delta/\Sigma t_i$ satisfactorily lies well within a small difference of ± 0.03 km/sec against the observed V_O, excepting a few cases. (See the last column). The division pattern thus depicted is shown in Fig. 4. Although this region-

5) *ibid.*, 3)

alization was made regarding the group velocity of Rayleigh waves with the period of 30 seconds, inasmuch as all the dispersion characters belong to a standard dispersion series, quite the same pattern can surely be drawn for group velocity data with other periods, in the range of 20-40 seconds at least[6]. Fig. 4, therefore, means the lateral variation of the dispersion character of Rayleigh waves.

4. Discussions and conclusions

The general view of the distribution pattern of dispersion regions shown in Fig. 4 is agreeable with the topography.

The most attractive evidence in Fig. 4 is that in the Canadian shield the dispersion character of Rayleigh waves has such a small index as 5.5. Group velocities of Rayleigh waves with this dispersion index are 3.20, 3.44, 3.59, 3.70 and 3.77 km/sec for the periods of 20, 25, 30, 35, 40 seconds respectively, which are nearly 7% higher than those for the dispersion index of 7 which is always found in the low land.

In the Canadian shield, J. Brune and J. Dorman derived a special crust-mantle model CANSD by the least squares inversion method from the phase velocity dispersions of both Love and Rayleigh waves[7]. In this model, shear waves velocity above and below the Moho is 3.85 km/sec and 4.72 km/sec respectively, which is remarkably higher than any of the corresponding values in other continental models. J. Brune et al. also observed the velocity of *Lg* phase covering the shield as 3.65 km/sec which is also considerably higher than the ordinary values of around 3.55 km/sec. In another paper[8], J. N. Brune also reported that *Sa* waves velocity due to the Hindu Kush Earthquake travelled through the Canadian shield was 4.55 km/sec, which is also higher than the mean values of that phase along other continental paths (4.49 km/sec) or in the tectonic region (4.40 km/sec). These high velocities of seismic waves above and below the Moho in the Canadian shield are well harmonized with the evidence for the relatively low value of heat flow in Quebee and Ontario[9].

---

6) *ibid.*, 1)

7) J. BRUNE and J. DORMAN., "Seismic Waves and Earth Structure in the Canadian Shield," *Bull. Seis. Scc. Amer.*, **53** (1963), 167-209.

8) J. N. BRUNE., "The Sa Phase from the Hindu Kush Earthquake of July 6, 1962," *Pure and Applied Geophys.*, **62** (1965), 81-95.

9) A. D. MIENER, L. G. D. THOMPSON and R. J. UFFEN," Terrestrial Heat Flow in Ontario and Quebee," *Trans. Amer. Geophys. U.*, **32** (1961), 729-738.

In the previous study[10], on the other hand, most of the African Continent and all of the Arabian Peninsula were found to have the dispersion index of *6* having the group velocities of Rayleigh waves nearly 5% higher than those of *7*. It was unexpected at that time that a dispersion region with such low dispersion index as *6* was found in the continent. This result, however, was well explained by suggesting a rather high velocity of seismic waves above and below the Moho. Referring to the study by J. Brune et al., it has since then been expected, therefore, that the dispersion index in the Canadian shield might be equal to or less than *6*.

The appearance of the dispersion region *5.5* in the Canadian shield in the present study fully satisfies the writer's expectation.

It is worthwhile to check the division pattern around the Canadian shield in Fig. 4 with the dispersion data obtained by J. Brune et al. In their paper, what can be compared directly with the present result is group velocity dispersion curve which they derived from the smoothed dispersion curve with regard to the phase velocities of Rayleigh waves

Table 5. Group velocity of Rayleigh waves for several periods T calculated from the division pattern along the paths used by J. Brune et al.

V in the lowest row indicates the group velocity which is read on a dispersion curve by J. Brune et al. having been derived from the smoothed dispersion curve of phase velocity.

T (sec) / Path	20	25	30	35	40
Res —Pal	2.94	3.20	3.36	3.51	3.61
Res —Ott	2.92	3.16	3.35	3.50	3.60
Res —Hal	3.02	3.29	3.44	3.57	3.65
Yuk—Pal	3.16	3.40	3.56	3.68	3.74
Hud—Pal	3.06	3.32	3.48	3.61	3.69
Arc —Pal	2.93	3.20	3.36	3.51	3.61
Arc —Ott	2.94	3.20	3.37	3.50	3.61
Hud—Res	3.01	3.27	3.43	3.57	3.65
mean	3.00	3.23	3.42	3.56	3.62
V	3.07	3.38	3.41	3.55	3.70

10) *ibid.*, 1)

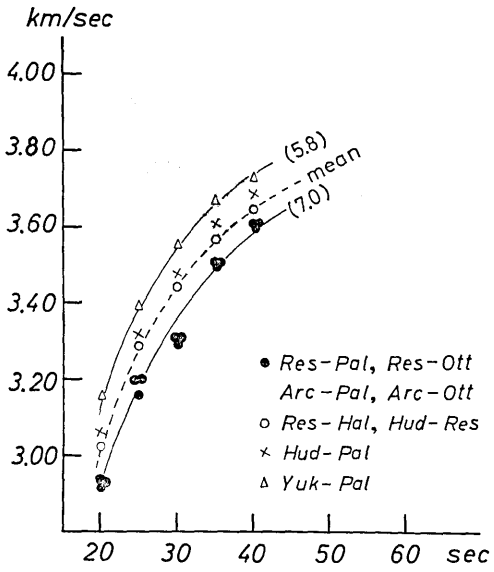

Fig. 5. Estimated group velocity dispersion data of Rayleigh waves along various paths used by J. Brune et al. basing upon the division pattern of dispersion regions.

along eight paths shown in Fig. 4. After J. Brune et al., phase velocity dispersion data along five paths, Yuk-Pal, Hud-Pal, Arc-Pal, Arc-Ott and Hud-Res lie on one curve excellently in such a wide period range as from 2 to 40 seconds (see Fig. 6 in their paper). It means that group velocity dispersion data along these paths also form exactly the same curve. This result, however, does not agree with the present one. From the topographical viewpoint only, more than half of the paths of Arc-Pal or Hud-Res, for instance, are occupied by a water-covered region, while the path of Yuk-Pal is a purely continental one. In our division map, the former contain the dispersion region *9* in Hudson Bay, while the latter passes mostly through the dispersion region *5.5*. Therefore, the dispersion data along these two kinds of paths cannot be the same. The group velocity of Rayleigh waves along eight paths are calculated as given in Table 5. Dispersion curves along every path thus obtained (Fig. 5) really varies from *6* to *7* in the dispersion indexes with such a large difference as nearly 0.2 km/sec in velocity scale.

Mean group velocities in Table 5, however, mostly coincide with those which are read on mean dispersion curve by J. Brune et al. having been derived from the phase velocity dispersion curve. Averaged dispersion character in the present paper, mixing the continental and water-covered areas in and around Canada, therefore, coincides with the model CANSD. However, inasmuch as a wide variation of dispersion character is suggested between the continental and water-covered areas, a new crust-mantle model for the purely continental part is required to be discovered at the first opportunity.

In Fig. 5, a small dispersion region *6* is revealed in the south-

western part of Lake Michigan. This small region was placed in order to explain the rather high group velocity of Rayleigh waves along the paths from a shock 14 to two stations 67 and 123. As is seen in Table 3(a), group velocity of Rayleigh waves with the period of 30 seconds along these paths are actually 3.41 km/sec and 3.42 km/sec respectively, which correspond to the dispersion index of less than 7. This dispersion region *6* seems to correspond to the location of the region with high *Pn* velocity of more than 8.4 km/sec which had been discovered by E. Herrin[11] et al. and by C. Romney et al.[12]

5. Dispersion data in and around the Arctic Ocean Basin

A preliminary trial was previously made[13] to divide the Arctic Ocean Basin into several regions with regard to the group velocity dispersion character of Rayleigh waves. At that time, however, the dispersion data were taken along the paths concentrated to only one station, Uppsala, Sweden, excepting two data by J. Oliver et al[14] along the paths to College, Alaska. The uniqueness of the pattern, therefore, had been remained to be checked. WWSSN offered many dispersion data of Rayleigh waves along various paths crossing well with each other (Fig. 6), which made it possible to revise the previous pattern above mentioned into a much more reliable one. Earthquake data are given in Table 1 (b) according to the preliminary epicenter determinations by USCGS.

As are shown in Fig. 7, dispersion data of Rayleigh waves crossing the Arctic Ocean lie well on the standard dispersion curves. In this figure, two facts must be emphasized here. The first is that two sets of dispersion data along the paths 6-52 (left diagram) and 16-52 (right diagram) lie on the standard curve with such a large index as *8* in spite of being purely oceanic paths. As will be made clear later, these facts are directly related to the existence of special dispersion region *10* around Novaya Zemlya which had been discovered[15] in the previous

11) E. HERRIN and J. TOGGART, "Regional Variations in Pn Velocity and Their Effect on the Location of Epicenters," *Bull. Seis. Soc. Amer.*, **52** (1962), 1037-1046.

12) C. ROMNEY, B. G. BROOKS, R. H. MANSFIELD, D. S. CARDER, J. N. JORDAN and D. W. GORDON, "Travel Time and Amplitudes of Principal Body Phases Recorded from GNOME," *Bull. Seism. Soc. Amer.*, **52** (1962), 1057-1074.

13) T. A. SANTÔ, "Dispersion of Surface Waves along Various Paths to Uppsala, Sweden. Part II. Arctic and Atlantic Ocean," *Annali di Geofisica*, **15** (1962), 277-298.

14) J. E. OLIVER, M. EWING and F. PRESS, "Crustal Structure of the Arctic Region from the Lg Phase," *Bull. Geol. Soc. Amer.*, **66** (1955), 1063-1074.

15) *ibid.*, 1)

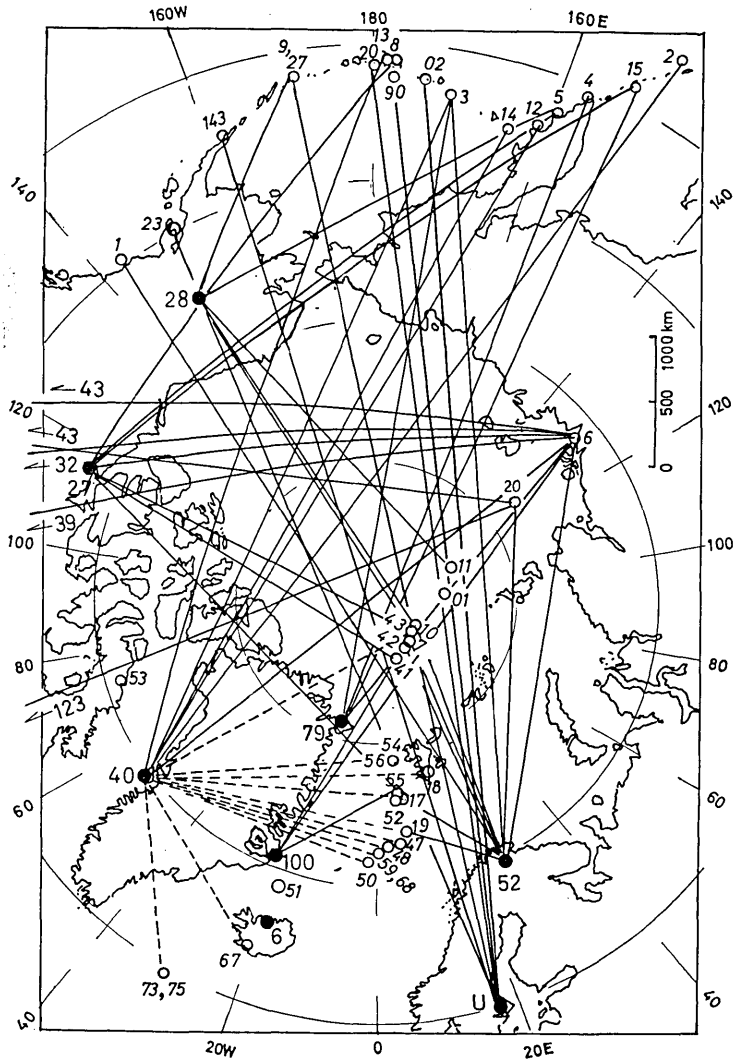

Fig. 6. Travelling paths of Rayleigh waves crossing the Arctic Ocean. The paths represented by dashed lines are those along which Rayleigh waves showed special characteristics.

study. The other fact is that dispersion data along the path 6-79 (Nord) lie parallel to the standard curve. The path 6-79 just runs over the seismic belt extended from the Mid-Atlantic belt. If this seismic belt is the extension of the special crust-mantle situation of the Mid-Atlantic

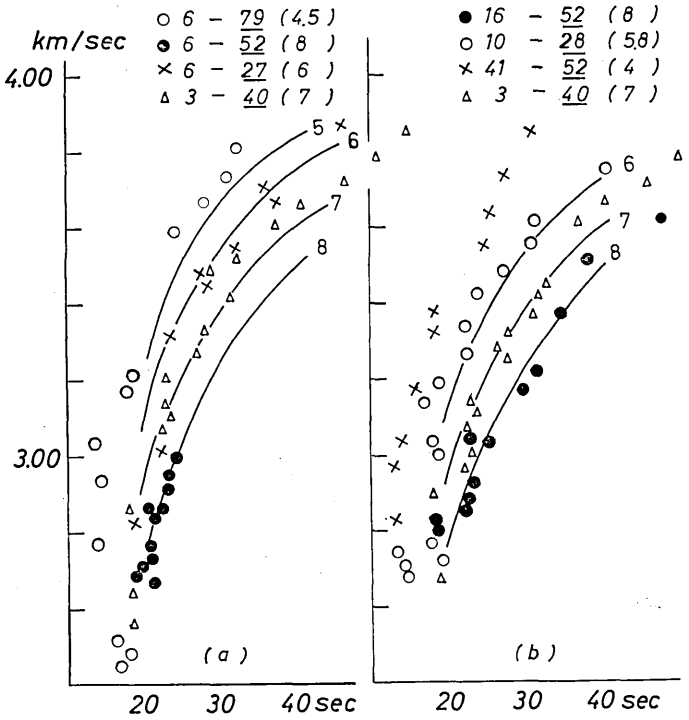

Fig. 7. Some examples of dispersion data of Rayleigh waves. Values in parenthesis mean the dispersion index along each measured by the standard curves.

Ridge, the dispersion character along the path 6-79 must show some of the special type with alphabet indexes which were observed along the Mid-Atlantic Ridge[16]. The present result was a negative one.

6. Regionalization of the Arctic Ocean Basin

Fig. 8 is a pattern of dispersion region which crossing-path technique revealed in the Arctic area with regard to the group velocity of Rayleigh waves. Table 6 gives the lengths of the segments (Δ_i) along every path cut by the pattern, and travel-times of Rayleigh waves along each segment (t_i). The new data of division on seven previous paths to Uppsala are also given in the last part of this Table. Comparison of calculated group velocity (V_c) basing upon the division pattern with the

16) *ibid.*, 3)

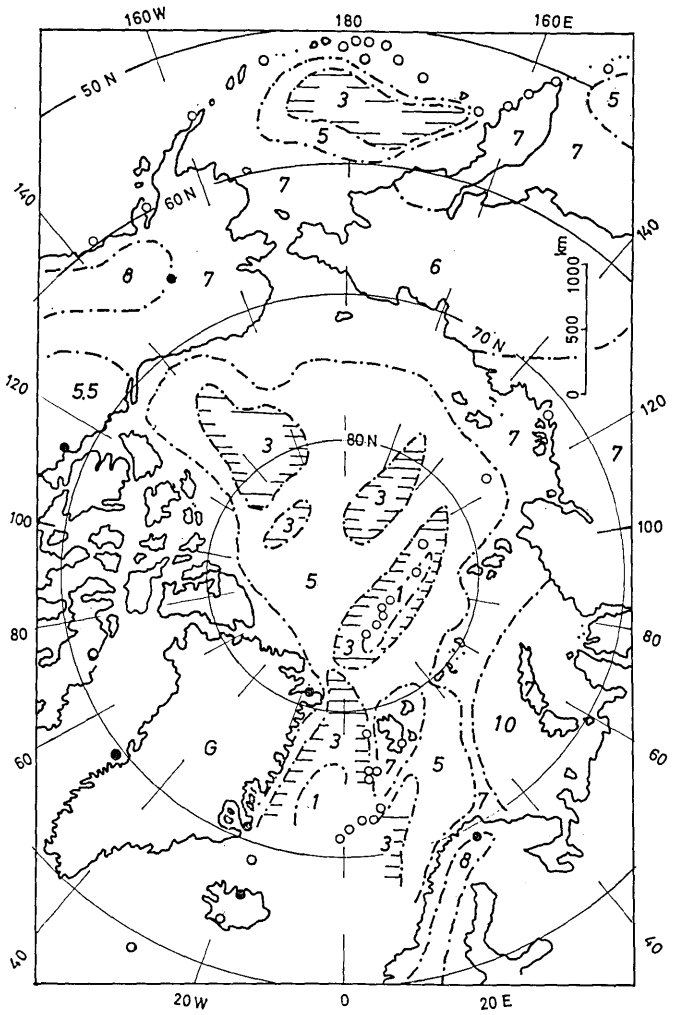

Fig. 8. Division pattern of dispersion region in and around the Arctic area.

observed value (V_0) is also made in the last column. Excepting one result along the path 18–79 showing an extremely large discrepancy, V_c agrees well with V_0 within a small difference of ± 0.03 km/sec.

Table 6. Divided segments Δ_i, travel-times of Rayleigh waves along each segment t_i, and the comparison of V_C with V_O. Paths are presented by the numberings of epicenter and station (underlined).

$t_i=\Delta_i/V_i$, where V_i is group velocity of Rayleigh with dispersion index i. $\Delta=\sum\Delta_i$, $C=\sum t_i$. O: Observed travel-times of Rayleigh waves along the total path. $V_C=\Delta/\sum t_i$. V_O: Observed group velocity of Rayleigh waves. (Period: 30 seconds)

Path	Travel-length Δ_i (in km) Travel-time t_i (in second) in segment								Δ	O C	V_O V_C	V_O-V_C
	1	*3*	*5*	*5.5*	*6*	*7*	*8*	*10*				
1- 52		1100	2150			1900	400		5550	1561	3.55	+0.00
		285	589			565	123			1562	3.55	
2- 40		500	2150	1500	1200	1700			7050	1956	3.60	+0.03
		129	587	410	341	505				1972	3.57	
3- 40		1000	500	300	400	3600			5800	1675	3.46	+0.00
		258	137	84	113	1070				1676	3.46	
3- 52		300	1700		800	3200			6000	1728	3.47	−0.01
		78	465		227	953				1723	3.48	
3- 79		300	2600		900	1100			4900	1371	3.57	0.00
		78	710		255	328				1371	3.57	
4- 79		1200	600		1000	2450			5250	1486	3.53	0.00
		311	164		284	727				1486	3.53	
5- 27			224		900	3550			4450	1310	3.40	+0.00
			0		255	1056				1311	3.40	
5- 28		1000				2150			3150	897	3.52	+0.00
		259				639				898	3.52	
6- 27		800	1200	300		1450			3750	1052	3.56	−0.01
		206	328	84		432				1050	3.57	
6- 32		400	1200	2000		4100			7700	2207	3.49	+0.01
		104	328	560		1221				2213	3.48	
6- 39		700	1000	3500		2100			7300	2050	3.56	+0.02
		180	273	980		625				2058	3.54	
6- 40		0	2250	1000		1000			4250	1186	3.58	+0.01
			614	280		298				1192	3.57	
6- 43		104	1500	1600		2700	1000		6800	1965	3.46	+0.01
		0	410	449		804	309			1972	3.45	
6- 52			300			1750		1300	3350	1034	3.24	+0.01
			82			520		435		1037	3.23	
6- 79	800	600	800			660			2860	782	3.66	+0.02
	200	156	224			197				777	3.68	
6-100	600	600	2000			950			4150	1133	3.66	+0.00
	150	156	546			283				1135	3.66	

(to be continued)

Table 6. (continued)

Path	Travel-length Δ_i (in km) Travel-time t_i (in second) in segment								Δ	O / C	V_O / V_C	V_O-V_C
	1	*3*	*5*	*5.5*	*6*	*7*	*8*	*10*				
7- 27		300	800	500		1170			2770	787	3.52	−0.02
		78	218	140		348				784	5.54	
7- 28		600	1400			700			3100	862	3.60	−0.02
		155	393			268				856	3.62	
7- 52	90	100	1000			700			1890	536	3.56	−0.01
	23	26	273			208				530	3.57	
8- 27		600	400	700		1700	500		3900	1130	3.45	−0.03
		155	109	196		506	154			1120	3.48	
9- 28						1600	300		1900	565	3.36	+0.02
						475	93			568	3.34	
10- 28		800	1430			800			3030	838	3.61	−0.00
		207	391			238				836	3.61	
10- 52	100	100	1180			600			1980	556	3.56	−0.03
	25	26	323			178				552	3.59	
10-100		1510		600					2100	555	3.79	0.00
		391		164						555	3.79	
11- 28		350	1250			1300			2900	822	3.53	−0.01
		91	341			386				818	3.54	
12- 40		800	200	400	700	3300			5800	1670	3.47	+0.01
		207	165	112	199	982				1665	3.46	
13- 40		400	1200	300		4000			5900	1713	3.44	−0.02
		155	274	84		1191				1704	3.46	
14- 40		800	800		400	3700			5700	1646	3.46	−0.02
		207	219		113	1100				1639	3.48	
15- 79		1200	800		1300	2200			5500	1546	3.56	+0.02
		311	218		369	655				1553	3.54	
15- 27					700	4400			5100	1510	3.38	−0.00
					199	1310				1509	3.38	
16- 43		800	1200	1700		2180	500		6380	1810	3.53	+0.00
		207	328	476		648	154			1813	3.53	
16-123		400	1400	2700		200			6100	1813	3.55	+0.01
		103	383	757		595				1838	3.54	
17- 27		400	400	1300		1550			3650	1035	3.53	+0.02
		104	109	364		461				1038	3.51	
17- 52		335	250			250	100		935	260	3.59	+0.01
		88	24			74	31			261	3.58	
18- 27		400	400	1300		1470			3570	1005	3.55	+0.03
		104	109	364		437				1014	3.52	
18- 52		500				437			937	261	3.58	−0.01
		130				130				260	3.59	
18- 79		400	88			300			788	212	3.72	+0.09
		104	24			89				217	3.63	

(to be continued)

Table 6. (continued)

Path	Travel-length Δi (in km) Travel-time t_i (in second) in segment								Δ	O C	V_O V_C	V_O-V_C
	1	*3*	*5*	*5.5*	*6*	*7*	*8*	*10*				
18-100	400	590	150			250			1390	367	3.79	+0.02
	100	153	41			75				369	3.77	
19- 52		255	250			150	150		805	228	3.53	−0.03
		67	68			45	46			226	3.56	
41- 27		200	800	500		1250			2750	782	3.52	0.00
		52	218	140		372				782	3.52	
41- 52	100	100	906			700			1880	502	3.60	−0.03
	25	26	248			208				507	3.57	
42- 28		600	1400	700					3100	857	3.62	−0.00
		155	393	208						856	3.62	
42- 27		300	800	500		1170			2770	785	3.53	−0.01
		78	218	140		343				784	3.54	
42- 52	100	100	900			780			1880	531	3.54	−0.01
			246			232				529	3.56	
43- 27		300	800	500		1180			2780	790	3.52	−0.01
		78	218	140		352				788	3.53	
44- 52		200	400			1320		800	2720	825	3.30	−0.01
		52	109			393		268		822	3.31	
45- 27					700	4400			5100	1510	3.38	−0.00
					199	1310				1509	3.38	
45- 79		1200	800		1300	2200			5500	1546	3.56	+0.02
		311	218		369	665				1553	3.54	

Path	Travel-length Δ_i (in km) Travel-time t_i (in second) in segment								Δ	O C	V_O V_C	V_O-V_C
	1	*3*	*5*	*5.5*	*6*	*7*	*8*	*10*				
U- 23		1200	3400			1600	500		6700	1865	3.60	+0.02
		311	930			476	154			1872	3.58	
U-143	100	800	2650			3500	200		7250	2050	3.54	+0.01
	25	207	725			1041	62			2060	3.53	
U- 27	100	700	3400			3160	200		7560	2129	3.55	+0.00
	25	181	927			94	62			2137	3.55	
U- 20	100	1300	2600		700	2660	200		7560	2120	3.57	+0.01
	25	337	710		199	790	62			2123	3.56	
U- 90	100	1200	1600		700	3630	200		7430	2124	3.50	−0.02
	25	311	438		199	1080	62			2115	3.52	
U- 02		800	1700		600	4100	200		7400	2111	3.50	+0.01
		207	465		170	1220	62			2124	3.49	
U- 01	100	150	700			2150	200		3300	953	3.46	−0.02
	25	39	191			640	62			957	3.48	

7. Special dispersion data along the paths containing Greenland

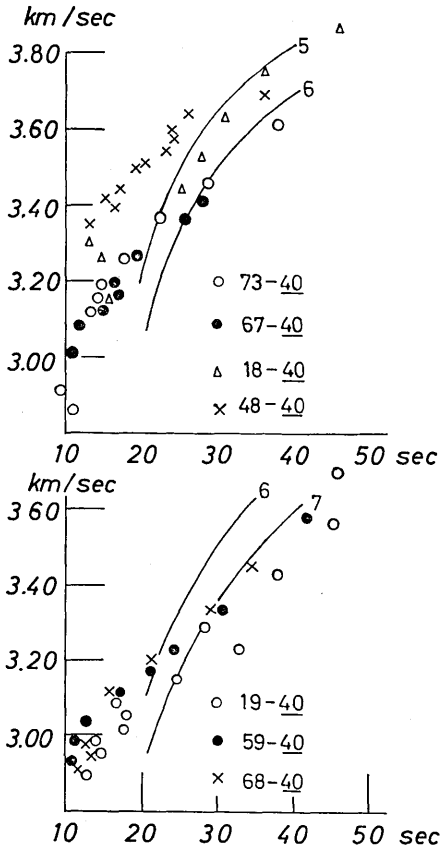

Fig. 9. Dispersion data of Rayleigh waves along the paths containing Greenland.

In section 3, it was pointed out that Rayleigh waves along the paths containing Greenland showed, without any exception, quite exceptional types, in which group velocities have a rather linear relation with the period. Group velocity dispersion data shown in Figs. 9 and 10 along many paths to a station 40 (dashed lines in Fig. 6) make the fact quite clear. These dispersion data are neither similar to the first special type which had been discovered along the Islands arcs just beside the trench[17] nor to the second one which had been obtained along the East Pacific Rise[18] and the Mid-Atlantic Ridge.

Rayleigh waves which arrived at a station 40 through Greenland showed another special feature. Relatively long period waves, larger than 50 seconds, developed well despite their rather short travelling distances of less than 2000 km. Usually, such was not the case.

As any reasons can hardly be suggested in the Greenland Sea which would specialize the dispersion character and promote the developement of long period Rayleigh waves in rather short travel-length, a thich ice sheet with average thickness of more that 2 km over Greenland may be responsible.

17) T. A. SANTÔ, "Observation of Surface Waves by Columbia-type Seismograph Installed at Tsukuba Station, Japan. (Part I)—Rayleigh Wave Dispersions across the Oceanic Basin, —" *Bull. Earthq. Res. Inst.*, **38** (1960), 219-240.

18) T. A. SANTÔ and M. BÅTH, "Crustal Structure of Pacific Ocean Area from Dispersion of Rayleigh Waves," *Bull. Seis. Soc. Amer.*, **53** (1963), 151-165

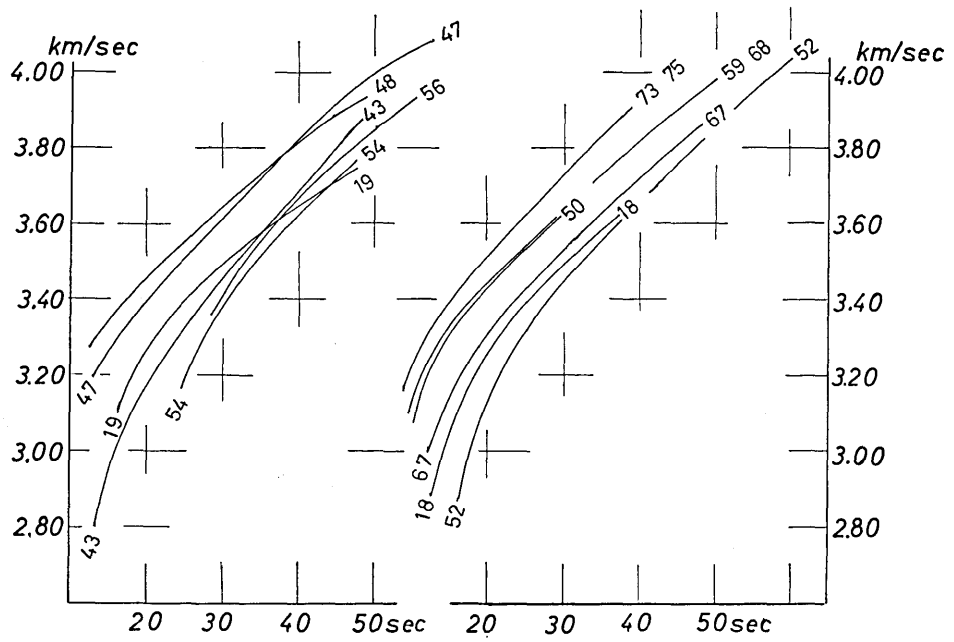

Fig. 10. Smoothed dispersion curves of Rayleigh waves crossing Greenland. Numerals beside every curve indicate the shock number corresponding to Fig. 6.

How does a thick ice sheet on Greenland change the dispersion of Rayleigh waves into so exceptional type? As it is desirable to get group velocity data along purely continental paths on Greenland, the problem above given must be left to be solved in the near future when a regionalization of dispersion regions in the neighbouring area, the Greenland Sea, is completed.

8. Discussions and conclusions

The bathymetry of the Arctic Ocean is not so deeply investigated as other oceanic areas where the approach is much easier. A bathymetric chart given in Fig. 11 may be one of the most reliable one which is drawn basing upon the chart constructed by N. A. Ostenso[19] on the basis of the works of a large number of individual investigators and scientific teams. Division pattern of dispersion region in Fig. 8 can be compared with the bathymetric chart. Purely oceanic dispersion regions

19) "Physiography and Structure of the Arctic Ocean Basin," *Trans. Amer. Geophys. U.*, 44 (1963), 637-648.

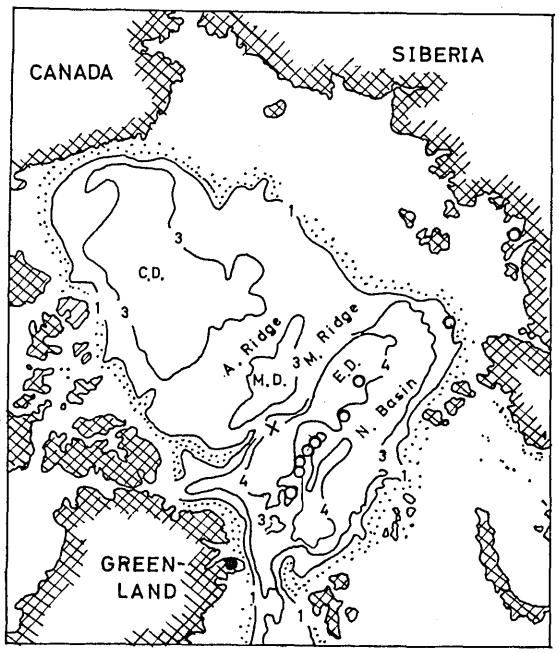

Fig. 11. Bathymetric chart in the Arctic Ocean. (Modified from the figure by N. A. Ostenso). For convenience of comparing with Fig. 8, epicenters along seismic belt through Arctic Ocean and a station 79 in Greenland are also shown by open and filled circles respectively. Pole is shown by cross mark.

with the dispersion index *3* between Canada and the North Pole exactly correspond to the Canada Deep which are reprensented by C. D. in the bathymetric chart. Eurasia Deep (E. D) and Nansen Basin (N. B.) in the bathymetric chart respectively corresponds to the oceanic indexes *1* and *3* in dispersion pattern. Markarov Deep (M. D.) in Fig. 11 also corresponds to the dispersion region *3* in Fig. 8 located between 140E and 180E, though the latter is somewhat swelled and its location is shifted to the south. The comparison tells that the pattern of dispersion region is, generally speaking, reasonably alike the bathymetric chart. The division pattern in the Bering Sea is also quite reasonable, comparing it with the bathymetric situation.

As has been mentioned in section 5, special attention must be paid to two points. The first is that the dispersion region around Novaya Zemlya which was characterised by such a large dispersion index as *10* was reconfirmed by the present data along the two paths to station 52 (Kevo) from two shocks of 6 and 44 (See Fig. 8 and Table 6). Actually, if the dispersion region *10* around Novaya Zemlya is replaced by the dispersion region *7* which is ordinarily found to exist in the continental shelf, the travel times of Rayleigh waves of 30 seconds periods from the epicenter 6 and 44 to 52 decrease 48 seconds and 30 seconds respectively, which makes such undesirable results with a large difference of V_c-V_0 as -0.15 km/sec and -0.21 km/sec respectively. The seconds point is that the dispersion data of Rayleigh waves travelling through or quite near a seismic belt from Greenland to northern Siberia did not show the

special dispersion character of alphabet type but showed ordinary standard type with rather oceanic index of approximately ***3.5***. (See Fig. 7).

As had been studied by L. R. Sykes,[20] the seismic belt in the Arctic Basin is characterized by its narrowness, and this seismic belt seem to be the extension of that of the Mid-Atlantic Ridge from its seismicity at least. Bathymetry in Fig. 11, however, does not show clearly the running of the Ridge over the seismic belt. Besides, as we have no data on heat flow, the high value of which characterizes the Mid-Oceanic Ridge, we still hesitate to comment on the geophysical similarity between the Arctic Ocean Ridge and the Mid-Atlantic Ridge. The similarity of the crust-mantle system of these two Ridges has also been an open question. Standard dispersion data obtained in the present study demands a normal crustal model along the Arctic Ocean Ridge, which is different from the Mid-Atlantic Ridge. Together with the similar negative results observed previously in the Indian Rise[21], the present evidence is worthwhile keeping in mind.

---

21. レイリー波群速度分散性の地理的分布 V: 北米大陸と北極海

地震研究所
国際地震・地震工学研修所 三東哲夫

これまでと同じ方法で，北米大陸と北極海をいくつかの分散区に分けてみた．北米大陸では，予想通り，カナダ楯状地が分散指数 **5.5** という，大陸としては大変に小さな値をもつ地区であることが明かになった (第 4 図)．唯，J. Brune らが，カナダ楯状地を代表する地殻マントルモデルとしてきめた CANSD モデルを見出すのに用いた分散資料を，こんど得た分散区の分布で検討してみると，分散指数 ***9*** を示すハドソン湾まで含んだ経路の資料も入っているので，CANSD は，カナダ楯状地だけのモデルとしては適当とは思えない．

北極海については，以前，スウェーデンのウプサラの記録を用いて分散区に分けたことあるが，こんどは，そのときの経路に交わるたくさんの道すぢにそつた分散資料が WWSSN の記録から得られ，以前の分散区の分布図はかなり詳しくかき改められた (第 8 図)．分散資料中に中央大西洋海嶺の延長と見られている浅発地震帯をちょうど含む経路上でのものがあつて，前に中央大西洋海嶺にそつて観測された異常分散性がこの経路上でも観測されるだろうと予想したが，その予想に反してそれは標準の分散曲線にのるものであった (第 7 図 (a) の白丸)．一方．ノバヤ・ゼムリヤ島周辺に大きな分散指数をもつ分散区があることが再確認された．また，これも前に報告したことであるが，グリーンランドを含んだ経路のレイリー波の分散は，今までに初めてみられる極めて特殊なものになる(第 10 図)ことも一層はっきりした．

20) L. R. Sykes, "The Seismicity of the Arctic," *Bull. Seis. Soc. Amer.*, **55** (1965), 519-536.

21) *ibid.*, 3)